Received: 3 January 2021 | Revised: 2 November 2021 | Accepted: 10 November 2021

DOI: 10.1111/cas.15205

ORIGINAL ARTICLE

Cancer Science WILEY

FGFR2 loss sensitizes MYCN-amplified neuroblastoma CHP134 cells to CHK1 inhibitor–induced apoptosis

Kiyohiro Ando[1,2,3,4] | Miki Ohira[1] | Ichiro Takada[5] | Verna Cázares-Ordoñez[5] | Yusuke Suenaga[3] | Hiroki Nagase[3] | Shinichi Kobayashi[4] | Tsugumichi Koshinaga[6] | Takehiko Kamijo[1] | Makoto Makishima[5] | Satoshi Wada[2,4]

[1]Research Institute for Clinical Oncology, Saitama Cancer Center, Saitama, Japan

[2]Department of Clinical Diagnostic Oncology, Showa University Clinical Research Institute for Clinical Pharmacology and Therapeutics, Tokyo, Japan

[3]Chiba Cancer Center Research Institute, Chiba, Japan

[4]Showa University Clinical Research Institute for Clinical Pharmacology and Therapeutics, Tokyo, Japan

[5]Division of Biochemistry, Department of Biomedical Sciences, Nihon University School of Medicine, Tokyo, Japan

[6]Department of Pediatric Surgery, Nihon University School of Medicine, Tokyo, Japan

Correspondence
Kiyohiro Ando, Research Institute for Clinical Oncology, Saitama Cancer Center, 818 Komuro, Ina, Kita-adachigun, Saitama, Japan.
Email: kiyohiro_ando@saitama-pho.jp

Funding information
This work was supported by JSPS KAKENHI (Grant Number JP18K07246).

Abstract

Checkpoint kinase 1 (CHK1) plays a key role in genome surveillance and integrity throughout the cell cycle. Selective inhibitors of CHK1 (CHK1i) are undergoing clinical evaluation for various human malignancies, including neuroblastoma. In this study, one CHK1i-sensitive neuroblastoma cell line, CHP134, was investigated, which characteristically carries *MYCN* amplification and a chromosome deletion within the 10q region. Among several cancer-related genes in the chromosome 10q region, mRNA expression of fibroblast growth factor receptor 2 (*FGFR2*) was altered in CHP134 cells and associated with an unfavorable prognosis of patients with neuroblastoma. Induced expression of *FGFR2* in CHP134 cells reactivated downstream MEK/ERK signaling and resulted in cells resistant to CHK1i-mediated cell growth inhibition. Consistently, the MEK1/2 inhibitor, trametinib, potentiated CHK1 inhibitor–mediated cell death in these cells. These results suggested that *FGFR2* loss might be prone to highly effective CHK1i treatment. In conclusion, extreme cellular dependency of ERK activation may imply a possible application for the MEK1/2 inhibitor, either as a single inhibitor or in combination with CHK1i in *MYCN*-amplified neuroblastomas.

KEYWORDS
CHK1 inhibitor, ERK, FGFR2, MEK inhibitor, neuroblastoma

1 | INTRODUCTION

Clinical heterogeneity in neuroblastoma has long been a subject of intense research because of an urgent need for improvement in the cure rate in high- and intermediate-risk groups, as well as mitigation of adverse effects by intensive multimodal therapy. Hence, several comprehensive analyses have been conducted to develop risk stratification, the International Neuroblastoma Risk Group (INRG) classification system, for heterogeneity of neuroblastoma biology.[1] The optimal treatment for patients with neuroblastoma has achieved consensus in the INRG Staging System.[2] Although amplified MYCN proto-oncogene (*MYCN*) and aberration of the long arm of chromosome 11 (11q aberration) are included in seven optimized prognostic risk factors in this system,[3] a series of altered gene expression and

Abbreviations: ATM, ataxia-telangiectasia mutated serine/threonine kinase; ATR, ataxia-telangiectasia mutated and Rad3-related serine/threonine kinase; CHK1, checkpoint kinase 1; CHK1i, CHK1 inhibitor; DDR, DNA damage response; MEK1/2i, MEK1/2 inhibitor; RS, replication stress; SD, standard deviation.

chromosome aberration contributes to the clinical heterogeneity of neuroblastoma. Other chromosome copy number aberrations in neuroblastomas, deletions of a distal part of the short arm of chromosome 1 (1p loss) and a gain of the long arm of chromosome 17 (17q gain), are recognized as hallmarks of worse outcomes in patients.[4] Additionally, recurrent losses within the distal 10q region have been observed in hereditary neuroblastoma, suggesting that a responsible gene preventing or predisposing to neuroblastoma may be harbored in this region.[5] It has been proposed that glioblastoma-related gene in 10q encoding deleted in malignant brain tumors 1 (*DMBT1*), fibroblast growth factor receptor 2 (*FGFR2*),[6] O-6-methylguanine-DNA methyltransferase (*MGMT*),[7] MAX-interacting protein 1 (*MXI1*),[8,9] and phosphatase and tensin homolog (*PTEN*) may also be responsible for the development of a small subset of neuroblastomas.[10-12] Silencing *MGMT* expression may sensitize neuroblastoma cells to the DNA methylating agent temozolomide[13]; however, other possible associations of 10q loss with neuroblastoma therapy are elusive.

FGFR2 is a tyrosine kinase receptor family member, and its alterations caused by gene amplification or mutations have been identified in various human cancers, including gastric, lung, breast, ovarian, endometrial, and cholangiocarcinoma.[14,15] There is no mutation in the *FGFR2* gene in neuroblastomas.[16] The increased expression of *FGFR2* confers cisplatin resistance on neuroblastoma cells by sequential activation of protein kinase C (PKC)-δ and inducing expression of antiapoptotic BCL2 and is associated with advanced stages of neuroblastoma.[17]

Checkpoint kinase 1 (CHK1) is responsible for the endogenous or exogenous DNA damage response (DDR), including replication fork licensing and cell cycle checkpoints, identifying it as a potential target for cancer therapy over the last decade.[18,19] As the observed efficacy of CHK1i in clinical trials of multiple human malignancies has been inadequate,[20-22] a key question with regard to the future application of a CHK1 inhibitor (CHK1i) for cancer therapy is which biomarker should be used to predict patients who would benefit from CHK1i treatment. Several studies have highlighted at least two remarkable factors that can influence the possible application of CHK1i therapy in various cancer preclinical models: (a) oncogene-induced replication stress (RS), as some cancer cells owe their oncogene-mediated hyperproliferation state to the so-called DNA replication checkpoint orchestrated by the ataxia-telangiectasia mutated and Rad3 related (ATR)-CHK1 axis,[23] and (b) the deficiency of homologous recombination repair (HRR), loss-of-function gene alterations in HRR genes, which enforces CHK1 dependency for cancer survival. Therefore, the cancer cells that possess these characteristic features may be vulnerable to CHK1i.[22] In line with this, we have recently reported that ataxia-telangiectasia mutated serine/threonine kinase (ATM) and DNA-PK inhibitors can overcome a low sensitivity to CHK1i in neuroblastoma cell lines with MYCN amplification, whereas the neuroblastoma CHP134 cell line is remarkably sensitive to CHK1i.[24]

In the present study, the CHP134 cell line was used to determine the factors contributing to CHK1i sensitivity. Our results revealed that decreased expression of *FGFR2* along with a loss of chromosome 10q was a key candidate feature contributing to CHK1i sensitivity in CHP134 cells. Furthermore, reintroduction of *FGFR2* activated MEK/ERK signaling and contributed to reduced CHK1i sensitivity while increasing sensitivity to MEK1/2 inhibitor (MEK1/2i). Therefore, a CHK1i and/or MEK1/2i may be a valuable therapeutic strategy to effectively treat certain types of *MYCN*-amplified neuroblastomas.

2 | MATERIALS AND METHODS

2.1 | Cell culture and inhibitors

The human neuroblastoma cell lines CHP134, NBLS, SKN-BE, SK-N-AS, IMR32, and SMS-SAN were purchased from the American Type Culture Collection and the RIKEN Bioresource Cell Bank, Tohoku University Cell Resource Center.[24,25] Cells were cultured in RPMI 1640 medium supplemented with 10% heat-inactivated FBS, 50 μg/mL penicillin, and 50 μg/mL streptomycin (Thermo Fisher Scientific). PF-477736 (a selective inhibitor of CHK1) and gemcitabine (GEM) or trametinib (GSK1120212, a selective inhibitor of MEK1/2) were purchased from Sigma Aldrich or Chemitek, respectively.

2.2 | Cell viability assays

Cells (20 000) were seeded into each well of a 96-well plate with 100 μL medium and incubated as described for the indicated times and conditions. Ten microliters of alamarBlue™ Cell Viability Regent (Invitrogen) were added to the cells for 1 hour, and immunofluorescence was measured using a SpectraMax M5e plate reader (Molecular Devices).

2.3 | Comparative genomic hybridization microarray (CGH-array)

For array-CGH (aCGH) analysis, 500 ng DNA from neuroblastoma cell lines or human placenta as a reference was fragmented and chemically labeled with Cy3- and Cy5-dyes, respectively. High-resolution aCGH was performed using the Agilent Human Genome CGH Microarray Kit 244K (Agilent Technologies) according to the manufacturer's protocol (Agilent Oligonucleotide Array-Based CGH for Genomic DNA Analysis, version 3.1 August 2009). Data was extracted from scanned microarray images using the Feature Extraction Software v11.0.1.1 (Agilent Technologies). Raw data were subsequently analyzed using Agilent Genomic Workbench Software (Agilent Technologies) and the ADM-2 algorithm with a threshold of 5.5.

2.4 | Quantitative reverse-transcription PCR of gene expression

Total RNA was isolated from the cells using an RNeasy mini kit (Qiagen) according to the manufacturer's procedure. Total RNA

was reverse-transcribed using random primers and Superscript II (Invitrogen) and then amplified on a StepOnePlus Real-Time PCR System with TaqMan Fast Universal PCR Master Mix to quantify expression of *FGFR2* and *ACTB* mRNA. FGFR2 and ACTB TaqMan probes (TaqMan Gene Expression Assay, Hs01552926_m1 and Hs01060665_g1, respectively) were purchased from Applied Biosystems.

2.5 | RNA-sequencing analysis

RNA sequencing (RNA-seq) data from human neuroblastoma CHP134 cell line (DRR062887), publicly available from the NCBI Sequence Read Archive, were downloaded. RNA-seq reads were aligned to the human genome (GRCh38.p12 downloaded from Ensembl Genome Browser) using HISAT2 (version 2.0.8) and then converted to bam files. mRNA expression of each gene was assessed using Broad's Integrated Genome Viewer (IGV 2.4).

2.6 | Construction of expression vectors and stable cell lines

The full-length cDNA for *FGFR2* was purchased from RIKEN (IRAK048H18). PCR amplification was performed using the cDNA template, and the product was subcloned into pENTR/D-TOPO (Invitrogen) to generate an entry clone. The forward and reverse primers used for PCR amplification were 5′- CACCATGGGATTAACGTCCACATG -3′ and 5′- TGTTTTAACACTGCCGTTTATGTGTG -3′. Generation of a stable cell line transduced with a lentiviral-mediated expression system was performed using the ViraPower Lentiviral Gateway Expression Kit (Invitrogen), as described previously.[26]

2.7 | CRISPR/Cas9-mediated gene editing

To ablate the *FGFR2* gene, TrueCut Cas9 Protein v2 (Invitrogen) and TrueGuide Synthetic gRNA targeting FGFR2 gene locus (CRISPR1089779_SGM, Invitrogen) were cotransfected into cells using Lipofectamine CRISPRMAX (Invitrogen) according to the manufacturer's instructions. Control cells were transfected with TrueCut Cas9 Protein v2 alone. The cells were incubated for 72 hours prior to analyses.

2.8 | Western blot analysis

Western blot analysis was performed as described previously.[24] Whole-cell extracts (50-100 μg protein) were separated using SDS-PAGE and were transferred to nitrocellulose membranes (Bio-Rad). Membranes were blocked and incubated with primary antibodies. Sixteen hours after incubation, the membranes were washed and incubated with HRP-coupled secondary antibodies. The proteins were developed using the ECL Western Blotting Detection Reagent (GE Healthcare). Signal intensities were detected by a ChemiDoc XRS+imaging system (GE Healthcare). The antibodies are listed in Appendix S1.

2.9 | Statistical analysis

Statistical analysis was performed using Microsoft Excel (Microsoft) and Statcel 4 (OMS Publishing). Statistical differences were analyzed using ANOVA followed by Scheffé's *F* test. The results are presented as the mean ± standard deviation (SD).

3 | RESULTS

3.1 | Genomic and genetic alteration of *FGFR2* was identified in CHK1 inhibitor–sensitive CHP134 cells

Recently, we investigated differential sensitivity to the CHK1 inhibitor (CHK1i), PF-477736, in four MYCN-amplified neuroblastoma cell lines and found that CHP134 cells are highly sensitive to CHK1i.[24] This prompted the investigation of CHP134 genomic and genetic features to identify a potential characteristic associated with the sensitivity to CHK1i. For this purpose, a CGH-array was performed to address genomic aberrations of CHP134 cell lines to compare these cells with other neuroblastoma cell lines. CHP134 cells possess 1p abnormality and chromosome gain of the *MYCN* locus (Figure 1A, purple and blue arrow, respectively).[27,28] Notably, among the dispersive chromosome aberrations, chromosome loss of the distal part of 10q (Figure 1A, red arrow) was discernable in CHP134 cells, as compared with the other neuroblastoma cell lines (Figure 1A,B). Next, it was determined if a genetic alteration was caused by the genomic aberration of 10q in CHP134 cells. The public RNA-seq database (DRR062887) was utilized to explore the alteration of mRNA expression of known cancer-related genes located in close vicinity to *FGFR2* (10q26.13): *MGMT* (10q.26.3), *MKI67* (10q26.2), and *PTEN* (10q23.31). As shown in Figure 1C, *FGFR2* mRNA expression was undetectable compared with other genes in the RNA-seq analysis. Furthermore, microarray analysis also failed to detect the expression of two of three probes designed within the coding sequences of *FGFR2* (chr10:123297866-123297807 and 123243276-123243217), and only feeble expression was captured using the other probe (chr10:123237843-123237830) (data not shown). These results indicated that *FGFR2* gene expression was silenced in CHP134 cells. The CGH analysis (Figure 1B) suggested that the CHP134 cells are not likely to be homozygous for the 10q deletion and may carry one copy of the 10q region, as previously shown in primary tumors and several neuroblastoma cell lines.[10] Therefore, it is plausible that epigenetic gene silencing, such as promoter hypermethylation of *FGFR2*, along with the loss of genomic regions, the so-called loss of heterozygosity (LOH), within 10q might downregulate *FGFR2* transcript levels, but not those of adjacent genes, *MGMT*, *MKI67*, and *PTEN*. Consistently, a recent comprehensive analysis showed that the expression levels

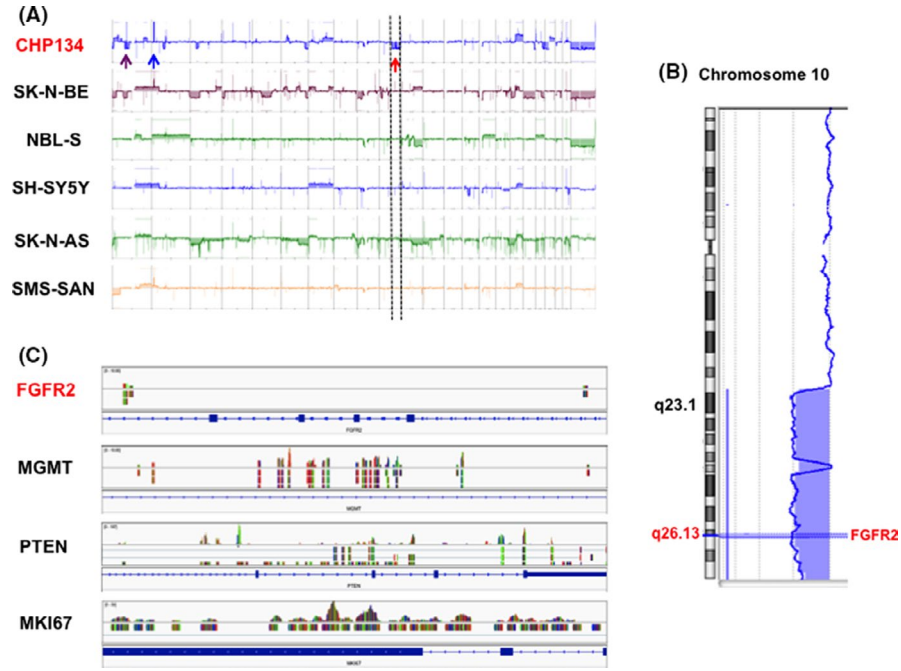

FIGURE 1 Partial loss of chromosome 10q results in alteration of *FGFR2* expression in CHP134 cells. A, Genomic signatures of six neuroblastoma cell lines using comparative genomic hybridization (CGH)-array. The colored histogram represents the rates of gains and losses for each clone, where the superior areas on the baseline correspond to gain and the inferior areas under the baseline correspond to loss. A red arrow indicates the partial loss of chromosome 10q. Purple and blue arrows indicate the 1p loss and gain of MYCN locus, respectively. B, Large image of partial chromosome loss of 10q. The *FGFR2* locus in 10q26.13 is depicted in the chromosome deletion (filled blue area). C, Expression signature of four cancer-associated genes located in chromosome 10q using RNA-sequencing analysis of the CHP134 cell line. Color images show detectable short-read RNA coverage of each gene locus

of *FGFR2* and downstream genes were negatively correlated with methylation in 32 cancer types.[29]

3.2 | *FGFR2* expression was associated with poor outcome in patients and cell growth in neuroblastoma

FGFR2 expression is significantly upregulated in stage 4 neuroblastomas, as well as *MYCN*-amplified neuroblastomas.[17] Consistently, the database analysis (R2, a Genomics Analysis and Visualization Platform) revealed that increased *FGFR2* expression was correlated with unfavorable prognosis in 88 neuroblastoma datasets (Versteeg-88-MAS5.0-u133p2, raw $P = .023$ and Bonferroni corrected $P = 1$, Figure 2A). To study the possible impact of *FGFR2* expression on neuroblastoma cell growth, a CHP134 cell line was introduced by lentiviral-mediated stable expression of the V5-tag–conjugated *FGFR2* (hereafter referred to as FGFR2 cells) along with V5-tag–conjugated *LACZ*-transduced cells as a control (hereafter referred to as LACZ cells), and then cell viability assays were performed (Figure 2B). As expected, FGFR2 cells significantly promoted cell growth compared with LACZ cells, suggesting that *FGFR2* had oncogenic potential in neuroblastoma. Interestingly, only a modest endogenous expression of FGFR2 protein was detected in CHP134, SK-N-BE, NBLS, and SMS-SAN cells, while it was clearly detectable in IMR32 cells and SK-N-AS (Figure 2C). In addition, induced expression of FGFR2 seemed to decrease the expression of both TP53 and MYCN, suggesting that transcriptional regulation by TP53 and/or MYCN might affect *FGFR2* expression in neuroblastoma. At the transcriptional levels, *FGFR2* mRNA was detected to various levels among cell lines (Figure 2D). Although FGFR2 protein was clearly detectable in SK-N-AS cells, the mRNA expression levels of FGFR2 in SK-N-AS cells was relatively downregulated compared with that in other cell lines, suggesting that the FGFR2 protein might be highly stable. These results indicated that the expression of FGFR2 might be caused not only by transcriptional regulation but also possibly by regulation at the post-transcriptional level.

3.3 | FGFR2 protected against CHK1i-mediated cell growth inhibition in CHP134 cells through the activation of MEK/ERK signaling

To further investigate the functional role of *FGFR2* in response to CHK1i, the cell viability of FGFR2 cells and LACZ cells with or without treatment with CHK1i, was assessed. In the present study, we utilized PF-477736 as a selective CHK1i.[24] Intriguingly, increased concentration of CHK1i remarkably inhibited cell viability in LACZ cells, whereas FGFR2 cells potently attenuated CHK1i-mediated cell growth inhibition (Figure 3A). The FGFR family has common key downstream pathways, such as the RAS–rapidly accelerated fibrosarcoma (RAF)–MAPK and the PI3K-AKT axis.[30] Next, the responsible pathway that was activated by the reintroduced expression

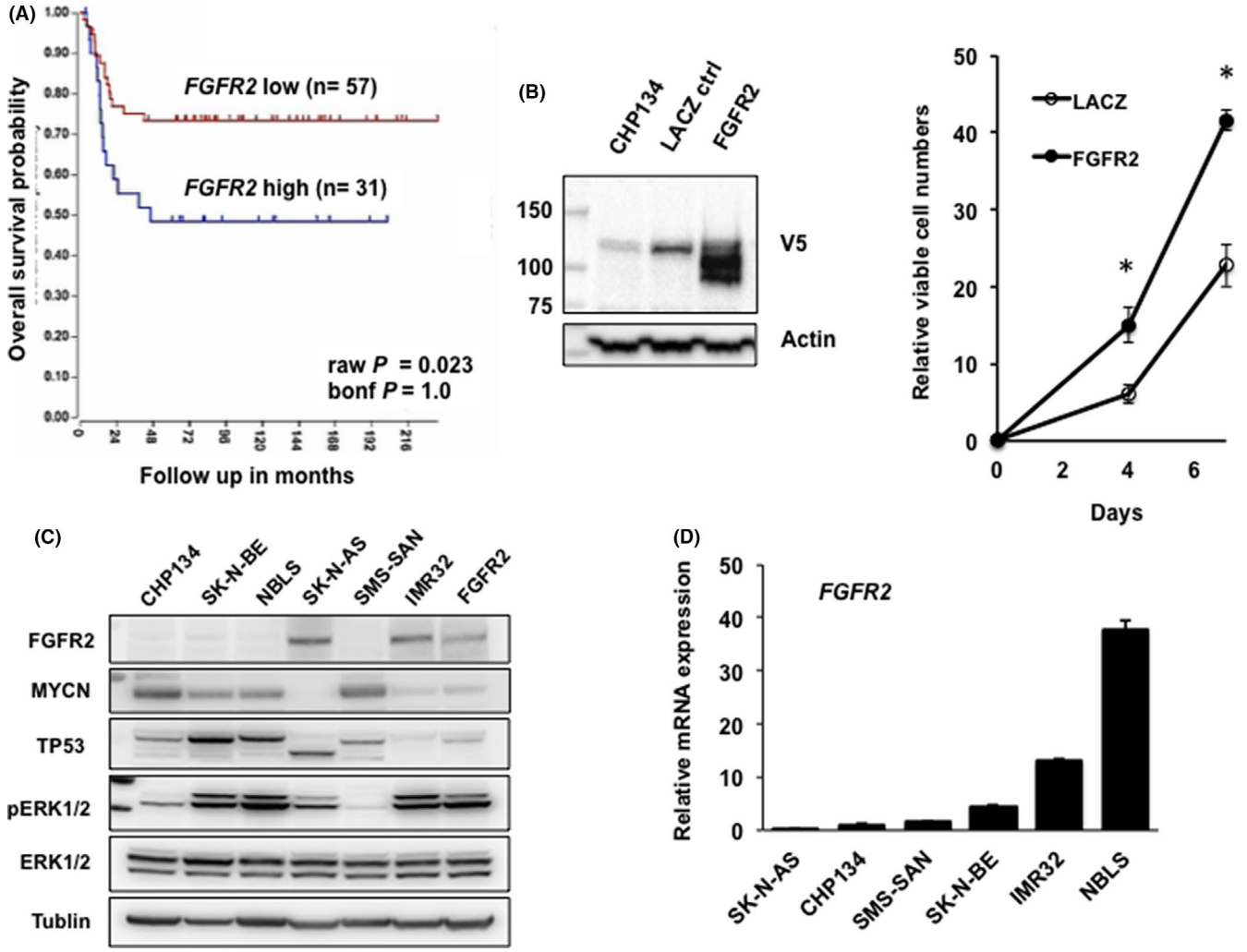

FIGURE 2 *FGFR2* expression is associated with an unfavorable prognosis and cell growth in neuroblastoma. A, Kaplan-Meier survival curves of a cohort of 88 patients with neuroblastoma stratified by high or low *FGFR2* mRNA expression. bonf *P*, Bonferroni-corrected *P*-value. B, Immunoblot analysis and cell viability assays for indicated cells. CHP134 cells are stably integrated with the V5-tag–conjugated *LACZ* gene (LACZ ctrl), the V5-tag–conjugated *FGFR2* gene (FGFR2), or are not lentivirally transduced (CHP134). Data are presented as the mean ± standard deviation (SD) of triplicates. $^*P < .01$. C, Immunoblot analysis of various neuroblastoma cell lines using the indicated antibodies. FGFR2, *FGFR2*-overexpressing CHP134 cells. D, quantitative RT-PCR analysis of *FGFR2* mRNA levels in neuroblastoma cell lines

of *FGFR2* was investigated. As indicated in Figure 3B, FGFR2 cells show increased ERK1/2 phosphorylation levels compared with those in LACZ cells, but there was no effect on AKT phosphorylation levels, suggesting the activation of the RAS-RAF-MAPK pathway. Consistently, as shown in Figure 3C, treatment with the MEK1/2i, trametinib, in FGFR2 cells restricts cell growth to certain levels (40%-50%) but has a limited effect in LACZ cells (10%-20%). In addition, ERK phosphorylation was elevated in CHK1i-insensitive SK-N-BE cells compared with that in CHP134 cells and SMS-SAN cells, both of which were categorized as CHK1i-sensitive cell lines (Figure 2C).[24]

To investigate the role of FGFR2 in CHK1i sensitivity, we genetically engineered *FGFR2*-ablated SK-N-AS and IMR32 cells using the CRISPR/Cas-9 system and assessed their sensitivity to CHK1i. As expected, *FGFR2*-ablated SK-N-AS cells decreased ERK phosphorylation and increased sensitivity to CHK1i (Figure 3D,E). In contrast, *FGFR2*-ablated IMR32 cells did not affect ERK phosphorylation or CHK1i sensitivity (Figure 3D,E). The FGFR2-independent activation of ERK in IMR32 cells may be causally related to multiple genetic alterations, such as ALK amplification and PKC activation, because the corresponding inhibitors moderately abrogated ERK activation (Figure S5A).[17,31,32] Taken together, these results suggest a crucial role of ERK activation in decreasing the sensitivity to CHK1i in neuroblastoma cells, regardless of FGFR2 expression.

3.4 | Combined blockade of CHK1 and ERK1/2 potentiated growth inhibition and apoptosis of neuroblastoma cells

Next, combination treatment with CHK1i and MEK1/2i was evaluated as a possible strategy for neuroblastoma therapy.

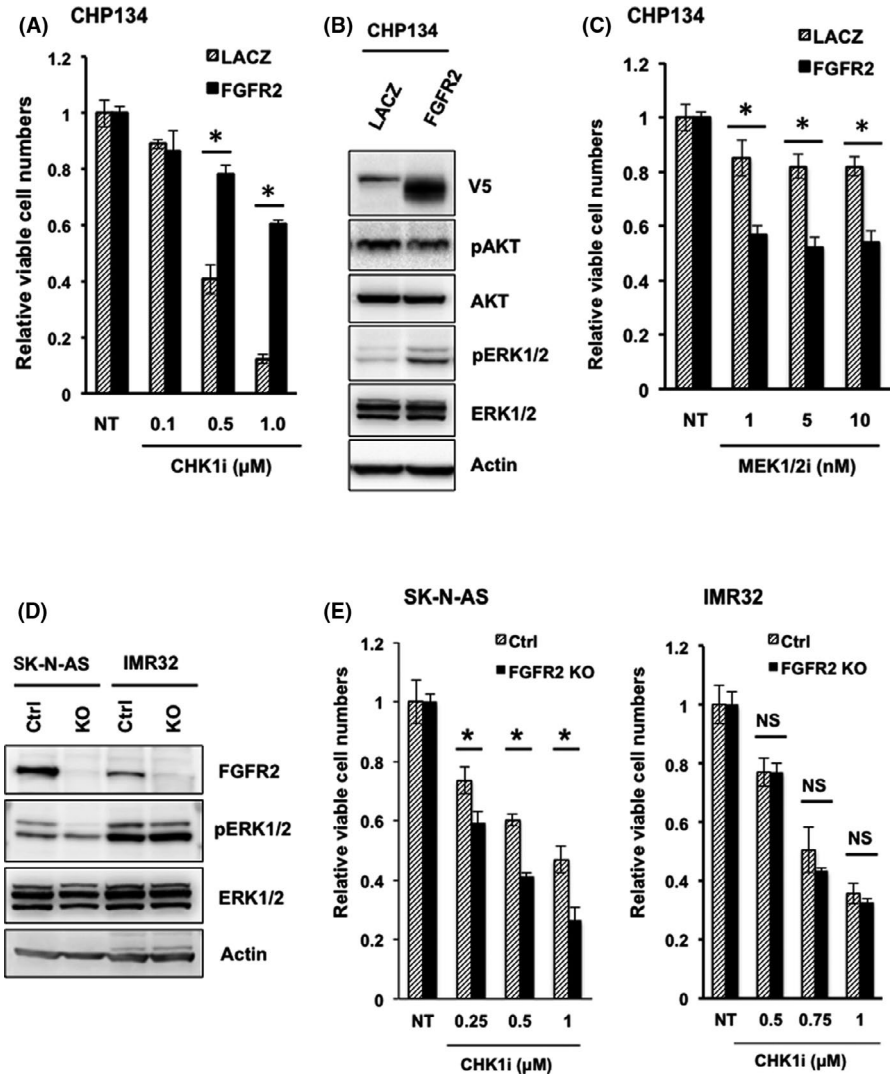

FIGURE 3 FGFR2 attenuates CHK1 inhibitor (CHK1i)-mediated inhibition of cell growth through ERK activation. A, E, Cell viability assays in V5-tagged *LACZ* or *FGFR2*-overexpressing CHP134 cells (LACZ or FGFR2 cells, respectively) and in SK-N-AS cells and IMR32 cells in which *FGFR2* is ablated or not (KO or Ctrl, respectively) after treatment with or without (NT) CHK1i (PF-477736) at the indicated concentrations for 48 h. B, D, Immunoblot analysis of the indicated protein in untreated LACZ and FGFR2 cells, SK-N-AS Ctrl and KO cells, IMR32 Ctrl and KO cells. C, Cell viability assays in LACZ and FGFR2 cells after treatment with MEK1/2 inhibitor (MEK1/2i, trametinib) at the indicated concentrations for 48 h. Relative viable cell numbers are normalized by those of the corresponding untreated cells. Statistical significance is presented as the mean ± standard deviation (SD) of triplicates. $^*P < .01$. NS, not significant

FGFR2-expressing or *FGFR2*-ablated neuroblastoma cells were treated with MEK1/2i in the presence or absence of CHK1i, and the cellular responses were assessed. As seen in Figure 4A, the efficacy of the combination treatment for cell growth inhibition was comparable to that of the single treatment with CHK1i in LACZ cells (see Figure 3A), whereas a synergistic effect between CHK1i and MEK1/2i was observed in FGFR2 cells (combination index,[33] 0.37). In detail, the combination treatment with 0.5 μmol/L CHK1i and 5 nmol/L MEK1/2i resulted in 55.0% inhibition of FGFR2 cell growth (Figure 4A), whereas the same levels of growth inhibition were achieved with 1.8 μmol/L CHK1i or 36.1 nmol/L MEK1/2i (Figure S1). Consistent with a previous report about tumor dependency on MEK activity,[34] PARP cleavage induced by the single-agent treatment with MEK1/2i was more notable in FGFR2 cells than in LACZ cells (Figure 4B, lanes 3 and 7). Thus, MEK1/2i might be a potential candidate for combination treatment with CHK1i to restore decreased sensitivity.

To further assess the mechanistic insights, levels of DNA damage and apoptotic induction in LACZ cells and FGFR2 cells treated with CHK1i and/or MEK1/2i were investigated. As shown in Figure 4B, MEK1/2i efficiently blocked ERK1/2 phosphorylation (lanes 3, 4, 7, and 8). As expected, treatment with CHK1i alone or the combination treatment with MEK1/2i induced DNA damage accumulation, as judged by the levels of histone variant phospho-histone H2A.X at Ser139 (γH2AX, lanes 2, 4, 6 and 8). The levels of DNA damage were lower in LACZ cells than in FGFR2 cells, suggesting the presence of more frequent massive apoptotic cell death with exhaustion of DDR in LACZ cells than in FGFR2 cells. Consistently, apoptotic induction detected by cleaved caspase-3 and cleaved PARP was slightly increased in LACZ cells compared with that in FGFR2 cells. Similarly, clonogenic survival at 6 days after combination treatment with MEK1/2i, the cells showed significant growth inhibition (Figure S2A) with apoptotic induction (Figure S2B) compared with that after single-agent treatment with CHK1i, whereas the levels of H2AX phosphorylation were comparably weak in both treatment conditions, suggesting exhaustion of DDR.

As previous findings showed that CHK1i strongly induced DDR in cells,[24] we determined whether the combined effect could be reproducible with a conventional DNA damage agent, GEM, instead of CHK1i. Combination treatment with 0.1 nmol/L GEM and 1 nmol/L MEK1/2i resulted in 51.3% inhibition of cell growth in FGFR2 cells (Figure S3A), whereas the same levels of growth inhibition were

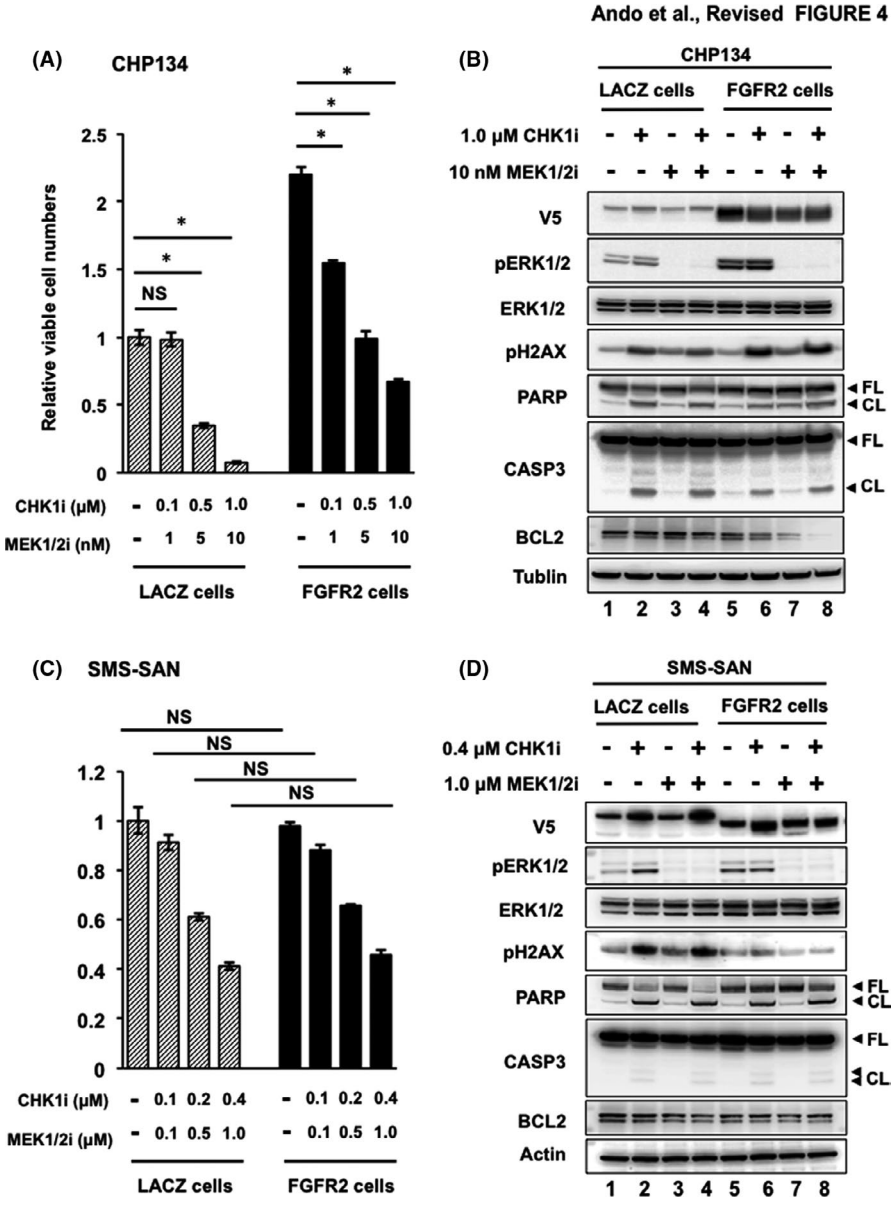

FIGURE 4 Combination blockade of CHK1 and MEK-ERK signaling efficiently inhibits cell growth in *FGFR2*-overexpressing CHP134 cells, but not in *FGFR2*-overexpressing SMS-SAN cells. A, C, Cell viability assays in LACZ and FGFR2 cells after treatment with CHK1i (PF-477736) and MEK1/2i (trametinib) at the indicated combination of each concentration for 48 h. Relative viable cell numbers obtained from all experimental conditions are normalized by those of untreated LACZ cells. Statistical significance is presented as the mean ± standard deviation (SD) of triplicates. $^*P < .01$. NS, not significant. B, D, Immunoblot analysis of the indicated protein in LACZ and FGFR2 cells after combination treatment with CHK1i and MEK1/2i at the indicated concentrations for 24 h. CL, cleaved form; FL, full-length

achieved with the single agents at 0.94 nmol/L GEM or 21.4 nmol/L MEK1/2i (Figures S1 and S3B), indicating synergistic effect between GEM and MEK1/2i (combination index, 0.15). Further investigation is needed to discriminate the therapeutic advantage of CHK1i from conventional cytotoxic agents for specific killing cancer cells and to reduce adverse side effects in patients.

To determine whether the combined effect applied to neuroblastoma cell lines other than CHP134 cells, we generated SMS-SAN cells, which overexpressed *FGFR2* or *LACZ* using a lentiviral-mediated stable expression system (Figure S4A). FGFR2-overexpressing SMS-SAN cells showed attenuated CHK1i sensitivity compared with the control LACZ cells (Figure S4B), whereas little or no increased sensitivity to MEKi or the combination treatment of CHK1i and MEKi, respectively, compared with the control cells (Figure S4C and Figure 4C). Interestingly, a slight apoptotic response was detected in both stable cells; γH2AX expression was attenuated only in FGFR2-overexpressing SMS-SAN cells (Figure 4D), suggesting that induced FGFR2 expression may contribute to activating survival signaling other than MEK-ERK in SMS-SAN cells. To elucidate the possible contribution of other survival signaling pathways in distinguishing the responses of FGFR2-overexpressing CHP134 cells and SMS-SAN cells, we assessed the expression of antiapoptotic BCL2 in response to the single or combination treatment.[17] Interestingly, FGFR2-overexpressing CHP134 cells, which are sensitive to MEK1/2i showed reduced expression of BCL2 in response to the singular treatment of MEK1/2i and its combination treatment with CHK1i (Figure 4B, lanes 7 and 8), whereas FGFR2-overexpressing SMS-SAN cells, which are relatively insensitive to MEK1/2i, did not alter BCL2 expression in response to either the singular or the combination treatment (Figure 4D, lanes 7 and 8). We further evaluated the combined effect of these inhibitors in IMR32 cells, which exhibit continuous activation of ERK in an FGFR2-independent manner, and in *FGFR2*-ablated SK-N-AS cells, in which ERK activation is abrogated. As expected, CHK1i-mediated cell growth inhibition was

further potentiated by MEK1/2i in IMR32 cells but not in FGFR2-ablated SK-N-AS cells (Figure 5A,B). We confirmed that BCL2 expression is abrogated in response to either MEK1/2i treatment alone or its combined treatment with CHK1i along with inducing apoptosis in IMR32 cells (Figure S5B).

Collectively, these results suggested that combination therapy of CHK1i and MEK1/2i might be effective in treating neuroblastomas. However, the efficacy of this therapeutic strategy could be profoundly affected by the cellular dependency of a cell survival signaling such as BCL2-mediated antiapoptotic signaling.

4 | DISCUSSION

The phase I study of PF-477736, a first generation of CHK1i, with GEM in adult patients with advanced solid malignancies (NCT00437203) was terminated due to business reasons, and therefore, the potential clinical benefits of this drug were not conclusively addressed. To date, several selective CHK1is, as well as inhibitors of its upstream DNA damage sensor kinase, ATR, have been developed in clinical trials.[35] Prexasertib (LY2606368), a second generation of CHK1i, has been evaluated in adult and pediatric patients with cancer.[36] Prexasertib exerts potent antiproliferative effects on cell lines and in xenograft mouse models of neuroblastoma.[37,38] Results from a phase I trial of prexasertib on pediatric patients with recurrent or refractory solid tumors (NCT02808650) were recently reported, but the therapeutic benefit in neuroblastoma patients remains inconclusive.[39] Notably, a phase II study (NCT02873975) evaluating the effects of prexasertib in adult patients with advanced solid tumors with RS or HRR deficiency is ongoing and will provide insight into the importance of those deficiencies for CHK1i sensitivity. It has been suggested that *MYCN* amplification be recognized as potentiating oncogene-induced RS, because c-MYC, the most noted MYC family member dysregulated in various cancers, plays essential roles in DNA replication.[40,41] The 11q loss, the other predictive marker for poor prognosis of neuroblastomas,[42] harbors four prominent genes responsible for faithful DNA replication and repairing double-strand breaks, *ATM*, *CHK1*, *MRE11*, and *H2AFX*, implicating genetic vulnerability of neuroblastomas to DDR-targeting agents, such as PARP inhibitors.[43,44] Remarkably, CHP134 cells have impaired ATM downstream signal activation by structural maintenance of chromosomes protein 1 (SMC1) phosphorylation, indicating partial deficiency of DDR.[44] Therefore, it is conceivable that CHP134 cells exhibiting *MYCN* amplification and ATM pathway deficiency are highly sensitive to CHK1i (Figure 5C). Importantly, FGFR2-overexpressing CHP134 cells showed decreasing sensitivity to CHK1i with ERK activation, suggesting the FGFR2-MEK-ERK axis may overcome the vulnerability attributed to either RS or HRR deficiency. Recent genomic deep-sequencing studies in relapsed neuroblastomas have revealed a clonally enriched somatic mutation converging on the RAS-MAPK pathway in

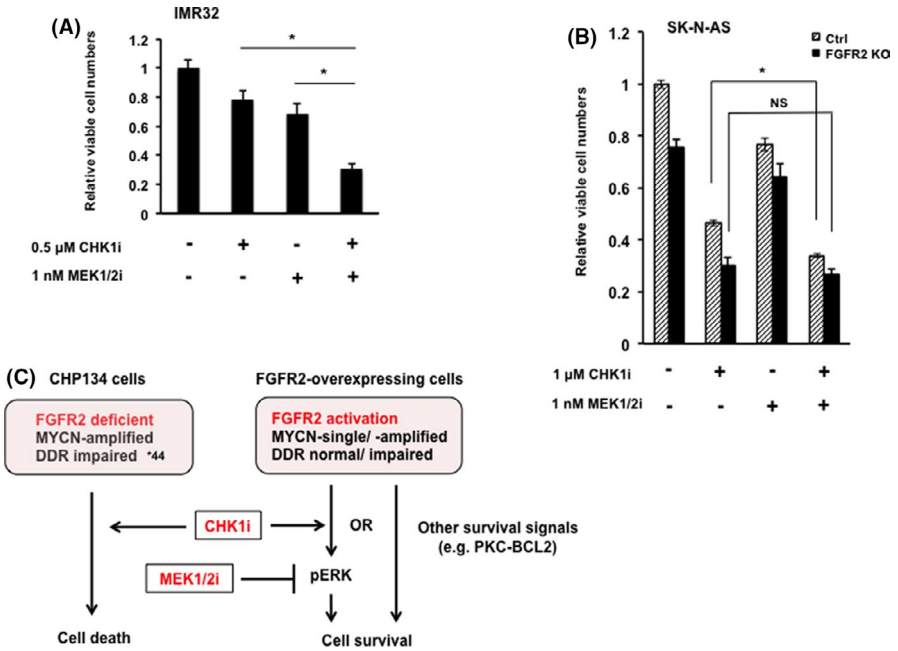

FIGURE 5 Differential effect of CHK1 inhibitor (CHK1i) and MEK1/2 inhibitor (MEK1/2i) in neuroblastoma cells with or without FGFR2 expression. A and B, Cell viability assays in IMR32 cells and SK-N-AS cells, in which *FGFR2* is ablated or not (FGFR2 KO or Ctrl, respectively) after treatment with CHK1i (PF-477736) and MEK1/2i (trametinib) at the indicated combination of each concentration for 48 h. Relative viable cell numbers are normalized by those of untreated IMR32 cells or the corresponding untreated SK-NAS cells. Statistical significance is presented as the mean ± standard deviation (SD) of triplicates. $^*P < .01$. NS, not significant. C, Schematic representation of the differential response to CHK1i and MEK1/2i in CHP134 cells or *FGFR2*-overexpressing cells. DDR impaired[*44], in 5C is described in Takagi et al.[44] DDR, DNA damage response

an activating manner,[45,46] and MEK inhibitors efficiently decrease tumor growth of mouse xenografts formed by neuroblastoma cell lines with RAS-MAPK mutations, SK-N-AS cells and NBL-S cells, suggesting clinical benefit for relapsed neuroblastomas.[45]

The idea of using CHK1i and MEK1/2i drug combination as a therapeutic strategy originally arose from in vitro studies on hematologic malignancies and prostate cancer, which demonstrated that CHK1i treatment induces ERK1/2 phosphorylation[47]; the present results are consistent with these observations (Figure 4B, lane 2). Further, 1 nmol/L MEK1/2i inhibited cell growth by 40%-50% in *FGFR2* cells (Figure 3C), whereas this efficacy was reduced to 30% in combination treatment with 0.1 μmol/L CHK1i (Figure 4A). Therefore, it is emphasized that neuroblastomas with aberrant activation of the RAS-MAPK pathway may not be recommended for single-agent therapy of CHK1i, but combination therapy with adequate concentrations of MEK1/2i should be preferred. Moreover, we observed that the sensitivity to either MEK1/2i alone or its combined treatment with CHK1i in FGFR2-overexpressing cells was associated to BCL2 expression. Taken together with the role of the FGFR2-PKC-BCL2 axis for cisplatin resistance in neuroblastomas,[17] PKC inhibitor may warrant consideration for neuroblastoma therapy.

In summary, the present study revealed that loss of *FGFR2* in neuroblastoma CHP134 cells, which have *MYCN* amplification and somewhat defective DDR, is responsible for CHK1i sensitivity, indicating the beneficial therapeutic role of CHK1i in neuroblastoma. Induced expression of *FGFR2* in CHP134 cells activated ERK1/2 and might protect cells from CHK1i-induced excessive DNA damage, but sensitized cells to MEK1/2i. However, sensitivity to MEK1/2i is more likely to be restricted by the cellular dependency of the survival pathways, such as antiapoptotic BCL2 signaling (Figure 5C); therefore, further studies are required to unveil the therapeutic implication of targeting the FGFR2-mediated signaling pathway in unfavorable neuroblastomas.

ACKNOWLEDGMENTS

We thank Editage (http://www.editage.com) for editing a draft of this manuscript.

DISCLOSURE

The authors disclose no potential conflicts of interest.

ORCID

Kiyohiro Ando https://orcid.org/0000-0002-2876-3304
Miki Ohira https://orcid.org/0000-0001-9105-1142
Hiroki Nagase https://orcid.org/0000-0002-3992-5399
Satoshi Wada https://orcid.org/0000-0001-6528-5914

REFERENCES

1. Cohn SL, Pearson AD, London WB, et al. The International Neuroblastoma Risk Group (INRG) classification system: an INRG Task Force report. *J Clin Oncol*. 2009;27:289-297.
2. Monclair T, Brodeur GM, Ambros PF, et al. The International Neuroblastoma Risk Group (INRG) staging system: an INRG Task Force report. *J Clin Oncol*. 2009;27:298-303.
3. Pinto NR, Applebaum MA, Volchenboum SL, et al. Advances in risk classification and treatment strategies for neuroblastoma. *J Clin Oncol*. 2015;33:3008-3017.
4. Nakagawara A, Li Y, Izumi H, Muramori K, Inada H, Nishi M. Neuroblastoma. *Jpn J Clin Oncol*. 2018;48:214-241.
5. Altura RA, Maris JM, Li H, Boyett JM, Brodeur GM, Look AT. Novel regions of chromosomal loss in familial neuroblastoma by comparative genomic hybridization. *Genes Chromosom Cancer*. 1997;19:176-184.
6. Fujisawa H, Kurrer M, Reis RM, Yonekawa Y, Kleihues P, Ohgaki H. Acquisition of the glioblastoma phenotype during astrocytoma progression is associated with loss of heterozygosity on 10q25-qter. *Am J Pathol*. 1999;155:387-394.
7. Nakamura M, Watanabe T, Yonekawa Y, Kleihues P, Ohgaki H. Promoter methylation of the DNA repair gene MGMT in astrocytomas is frequently associated with G: C –> A: T mutations of the TP53 tumor suppressor gene. *Carcinogenesis*. 2001;22:1715-1719.
8. Wechsler DS, Shelly CA, Petroff CA, Dang CV. MXI1, a putative tumor suppressor gene, suppresses growth of human glioblastoma cells. *Can Res*. 1997;57:4905-4912.
9. Albarosa R, DiDonato S, Finocchiaro G. Redefinition of the coding sequence of the MXI1 gene and identification of a polymorphic repeat in the 3' non-coding region that allows the detection of loss of heterozygosity of chromosome 10q25 in glioblastomas. *Hum Genet*. 1995;95:709-711.
10. Lazcoz P, Munoz J, Nistal M, Pestana A, Encio IJ, Castresana JS. Loss of heterozygosity and microsatellite instability on chromosome arm 10q in neuroblastoma. *Cancer Genet Cytogenet*. 2007;174:1-8.
11. Munoz J, Lazcoz P, Inda MM, et al. Homozygous deletion and expression of PTEN and DMBT1 in human primary neuroblastoma and cell lines. *Int J Cancer*. 2004;109:673-679.
12. Bello MJ, Alonso ME, Aminoso C, et al. Hypermethylation of the DNA repair gene MGMT: association with TP53 G: C to A: T transitions in a series of 469 nervous system tumors. *Mutat Res*. 2004;554:23-32.
13. Wagner LM, McLendon RE, Yoon KJ, Weiss BD, Billups CA, Danks MK. Targeting methylguanine-DNA methyltransferase in the treatment of neuroblastoma. *Clin Cancer Res*. 2007;13:5418-5425.
14. Katoh M. Cancer genomics and genetics of FGFR2 (Review). *Int J Oncol*. 2008;33:233-237.
15. Mahipal A, Tella SH, Kommalapati A, Anaya D, Kim R. FGFR2 genomic aberrations: Achilles heel in the management of advanced cholangiocarcinoma. *Cancer Treat Rev*. 2019;78:1-7.
16. Shukla N, Ameur N, Yilmaz I, et al. Oncogene mutation profiling of pediatric solid tumors reveals significant subsets of embryonal rhabdomyosarcoma and neuroblastoma with mutated genes in growth signaling pathways. *Clin Cancer Res*. 2012;18:748-757.
17. Salm F, Cwiek P, Ghosal A, et al. RNA interference screening identifies a novel role for autocrine fibroblast growth factor signaling in neuroblastoma chemoresistance. *Oncogene*. 2013;32:3944-3953.
18. Dai Y, Grant S. New insights into checkpoint kinase 1 in the DNA damage response signaling network. *Clin Cancer Res*. 2010;16:376-383.
19. Merry C, Fu K, Wang J, Yeh IJ, Zhang Y. Targeting the checkpoint kinase Chk1 in cancer therapy. *Cell Cycle*. 2010;9:279-283.
20. Hong DS, Moore K, Patel M, et al. Evaluation of prexasertib, a checkpoint kinase 1 inhibitor, in a Phase Ib study of patients with squamous cell carcinoma. *Clin Cancer Res*. 2018;24:3263-3272.
21. Lee JM, Nair J, Zimmer A, et al. Prexasertib, a cell cycle checkpoint kinase 1 and 2 inhibitor, in BRCA wild-type recurrent high-grade serous ovarian cancer: a first-in-class proof-of-concept phase 2 study. *Lancet Oncol*. 2018;19:207-215.
22. Lin AB, McNeely SC, Beckmann RP. Achieving precision death with cell-cycle inhibitors that target DNA replication and repair. *Clin Cancer Res*. 2017;23:3232-3240.

23. Toledo L, Neelsen KJ, Lukas J. Replication catastrophe: when a checkpoint fails because of exhaustion. *Mol Cell*. 2017;66:735-749.
24. Ando K, Nakamura Y, Nagase H, et al. Co-Inhibition of the DNA damage response and CHK1 enhances apoptosis of neuroblastoma cells. *Int J Mol Sci*. 2019;20(15):3700.
25. Takenobu H, Shimozato O, Nakamura T, et al. CD133 suppresses neuroblastoma cell differentiation via signal pathway modification. *Oncogene*. 2011;30:97-105.
26. Ando K, Cazares-Ordonez V, Makishima M, et al. CEP131 abrogates CHK1 inhibitor-induced replication defects and is associated with unfavorable outcome in neuroblastoma. *J Oncol*. 2020;2020:2752417.
27. Fulda S, Honer M, Menke-Moellers I, Berthold F. Antiproliferative potential of cytostatic drugs on neuroblastoma cells in vitro. *Eur J Cancer*. 1995;31A:616-621.
28. Brodeur GM, Green AA, Hayes FA, Williams KJ, Williams DL, Tsiatis AA. Cytogenetic features of human neuroblastomas and cell lines. *Can Res*. 1981;41:4678-4686.
29. Li J, Hu K, Huang J, Zhou L, Yan Y, Xu Z. A pancancer analysis of the expression landscape and clinical relevance of fibroblast growth factor receptor 2 in human cancers. *Front Oncol*. 2021;11:644854.
30. Turner N, Grose R. Fibroblast growth factor signalling: from development to cancer. *Nat Rev Cancer*. 2010;10:116-129.
31. Fransson S, Hansson M, Ruuth K, et al. Intragenic anaplastic lymphoma kinase (ALK) rearrangements: translocations as a novel mechanism of ALK activation in neuroblastoma tumors. *Genes Chromosom Cancer*. 2015;54:99-109.
32. Subramonian D, Phanhthilath N, Rinehardt H, et al. Regorafenib is effective against neuroblastoma in vitro and in vivo and inhibits the RAS/MAPK, PI3K/Akt/mTOR and Fos/Jun pathways. *Br J Cancer*. 2020;123:568-579.
33. Chou TC. Drug combination studies and their synergy quantification using the Chou-Talalay method. *Can Res*. 2010;70:440-446.
34. Solit DB, Garraway LA, Pratilas CA, et al. BRAF mutation predicts sensitivity to MEK inhibition. *Nature*. 2006;439:358-362.
35. Pilie PG, Tang C, Mills GB, Yap TA. State-of-the-art strategies for targeting the DNA damage response in cancer. *Nat Rev Clin Oncol*. 2019;16:81-104.
36. Angius G, Tomao S, Stati V, Vici P, Bianco V, Tomao F. Prexasertib, a checkpoint kinase inhibitor: from preclinical data to clinical development. *Cancer Chemother Pharmacol*. 2020;85:9-20.
37. Lowery CD, Dowless M, Renschler M, et al. Broad spectrum activity of the checkpoint kinase 1 inhibitor prexasertib as a single agent or chemopotentiator across a range of preclinical pediatric tumor models. *Clin Cancer Res*. 2019;25(7):2278-3228.
38. Lowery CD, VanWye AB, Dowless M, et al. The checkpoint kinase 1 inhibitor prexasertib induces regression of preclinical models of human neuroblastoma. *Clin Cancer Res*. 2017;23:4354-4363.
39. Cash T, Fox E, Liu X, et al. A phase 1 study of prexasertib (LY2606368), a CHK1/2 inhibitor, in pediatric patients with recurrent or refractory solid tumors, including CNS tumors: a report from the Children's Oncology Group Pediatric Early Phase Clinical Trials Network (ADVL1515). *Pediatr Blood Cancer*. 2021;68:e29065.
40. Dominguez-Sola D, Gautier J. MYC and the control of DNA replication. *Cold Spring Harb Perspect Med*. 2014;4:a014423.
41. Dominguez-Sola D, Ying CY, Grandori C, et al. Non-transcriptional control of DNA replication by c-Myc. *Nature*. 2007;448:445-451.
42. Attiyeh EF, London WB, Mosse YP, et al. Chromosome 1p and 11q deletions and outcome in neuroblastoma. *N Engl J Med*. 2005;353:2243-2253.
43. Southgate HED, Chen L, Curtin NJ, Tweddle DA. Targeting the DNA damage response for the treatment of high risk neuroblastoma. *Front Oncol*. 2020;10:371.
44. Takagi M, Yoshida M, Nemoto Y, et al. Loss of DNA damage response in neuroblastoma and utility of a PARP inhibitor. *J Natl Cancer Inst*. 2017;109(11). http://dx.doi.org/10.1093/jnci/djx062
45. Eleveld TF, Oldridge DA, Bernard V, et al. Relapsed neuroblastomas show frequent RAS-MAPK pathway mutations. *Nat Genet*. 2015;47:864-871.
46. Li Y, Ohira M, Zhou Y, et al. Genomic analysis-integrated whole-exome sequencing of neuroblastomas identifies genetic mutations in axon guidance pathway. *Oncotarget*. 2017;8:56684-56697.
47. Tang Y, Dai Y, Grant S, Dent P. Enhancing CHK1 inhibitor lethality in glioblastoma. *Cancer Biol Ther*. 2012;13:379-388.

SUPPORTING INFORMATION

Additional supporting information may be found in the online version of the article at the publisher's website.

How to cite this article: Ando K, Ohira M, Takada I, et al. FGFR2 loss sensitizes MYCN-amplified neuroblastoma CHP134 cells to CHK1 inhibitor–induced apoptosis. *Cancer Sci*. 2022;113:587–596. doi:10.1111/cas.15205